Optical spectra of free silver clusters and microcrystal produced by the gas evaporation technique: transition from atom to microcrystal



1993 J. Phys.: Condens. Matter 5 135

(http://iopscience.iop.org/0953-8984/5/1/015)

J. Phys.: Condens. Matter 5 (1993) 135–144. Printed in the UK

# Optical spectra of free silver clusters and microcrystals produced by the gas evaporation technique: transition from atom to microcrystal

Shōsuke Mochizuki† and Raphael Ruppin‡

† Department of Physics, College of Humanities and Sciences, Nihon University, 3-25-40 Sakurajosui, Setagaya-ku, Tokyo 156, Japan

‡ Department of Applied Physics and Mathematics, Soreq Nuclear Research Centre, Yavne 70600, Israel

Received 27 March 1992, in final form 11 August 1992

**Abstract.** By setting an appropriate condition for the gas evaporation of silver, two vertically well separated zones—a transparent emission zone and a bright smoky zone—have been produced above the evaporation source in a confined helium atmosphere. Optical data were obtained by measuring time-resolved and space-resolved transmissivity spectra. The structure of the spectra and their dependence on time on the one hand and on the distance from the source on the other hand support the occurrence of atoms, clusters and microcrystals. The mechanism of the growth of silver clusters and microcrystals by the gas evaporation technique is also studied.

## 1. Introduction

In recent years, considerable attention has been given to the theoretical and experimental investigation of the physical and chemical properties of clusters and microcrystals. The question of how the electronic and vibrational states change with increasing number of constituent atoms is of great interest. However, because of the difficulties of measurement, most of the experiments are concentrated on either microclusters containing only a small number of atoms or on microcrystals larger than several nanometres. Thus, information on the transition of the physical properties with increasing number of atoms over a wide region of cluster sizes is still incomplete. In recent work on the transition from atoms to microcrystals (Welker and Martin 1979, Schulze *et al* 1978), the optical properties of metal clusters of various sizes have been measured using the matrix isolation technique, in which metallic species (atoms, clusters and microcrystals) are embedded in a noble-gas matrix. The average metal cluster size was controlled by varying the concentration of the metal vapour used in the process. However, in the interpretation of the spectra the difficulty of including the effect of the noble-gas matrix is encountered. Thus, it seems advantageous to measure the optical properties of the various species without embedding them in a matrix. This has recently been achieved in our laboratory (Mochizuki 1991, 1992) by employing time-resolved and space-resolved spectroscopies of Ag or Na vapours from an evaporation source in a helium gas atmosphere. In the present paper we report the details of these experiments and present optical spectra which demonstrate

0953-8984/93/010135+10$07.50  

the transition from atoms to clusters to microcrystals. We identify the discrete lines appearing in the spectra, as well as the collective mode resonance and discuss the growth mechanism of the clusters and microcrystals in gas evaporation.

## 2. Experimental details

It is well known that metal aggregates with various sizes between several Ångströms and several microns can be produced easily by thermal evaporation without any nozzle under a low-pressure noble gas (see, e.g., Ueda 1974, Granqvist and Buhrman 1976). This method is called the 'gas evaporation method'. The structure of the vapour zone produced above an evaporation source by the gas evaporation method depends on the size and shape of the evaporation source, the pressure and flow rate of the gas, the evaporation temperature, etc. Thus, by setting appropriate experimental conditions, we are able to produce two separate zones at different heights above the evaporation source, one containing atoms and clusters and another containing microcrystals. Figure 1 shows a typical view of the gas evaporation of silver in the confined helium gas at 140 Torr. This figure was taken without illumination. A nearly transparent zone ranging from the upper edge of the crucible to a height of about 8 mm, and a long and bright smoky zone can be clearly distinguished. The nearly transparent zone and the smoky zone appear as violet and white, respectively, to the naked eye. The colours of the emitted and scattered light are specific to each metal (Eversole and Broida 1977, Hayashi *et al* 1977, Saito 1989, Mochizuki 1992). The violet and the bright smoky-white zones are the emission from metal species and the scattered light of the thermal emission from the evaporation source at high temperatures. It was found that, with decreasing pressure of the helium gas or with decreasing temperature of the crucible, or with increasing flow rate of the helium gas, it becomes difficult to distinguish these zones. Since we have observed intense light scattering in the smoky zone, while we have scarcely observed such light scattering in the transparent zone, it may be assumed that the transparent zone contains silver species with a small number of constituent atoms, while the smoky region contains larger clusters and microcrystals. It is therefore possible to obtain optical spectra of species of increasing size by performing a vertical scan, beginning at the lower part of the transparent zone and moving up into the smoky zone. Moreover, time-resolved spectroscopy can be performed at a fixed height in the various zones. This can be performed from the beginning of the evaporation until a steady state is reached. The growths of dimers, small clusters, large clusters and microcrystals with time can be monitored by this method. Of course, the ultimate maximum cluster size at steady state increases with increasing height at which the time-resolved measurements are performed. This combination of both time-resolved and space-resolved measurement provides a very useful technique for the observation of the whole range of species sizes, without using complicated experimental apparatus.

Time-resolved transmission spectra were recorded in the spectral region from 230 to 800 nm at heights ranging from the upper edge of the crucible up to 25 mm. A block diagram for the experiment is given in figure 2. Except for the measurement on the microcrystal beam which will be described in the last part of the results, gas evaporation was carried out in confined helium gas at 140 Torr above 1800 K by electrically heating high-purity silver in an alumina crucible on which was wound a tungsten-wire heater. The temperature of the crucible was gradually increased by

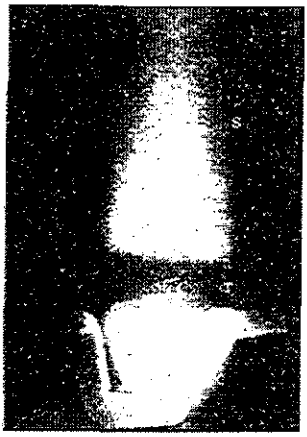


**Figure 1.** Well separated zone structure of the gas evaporation of silver above 1800 K in a confined helium gas at 140 Torr. A nearly transparent zone T extends from the upper edge of the crucible C to a height of about 8 mm and a bright smoky zone S appears white above the nearly transparent zone.

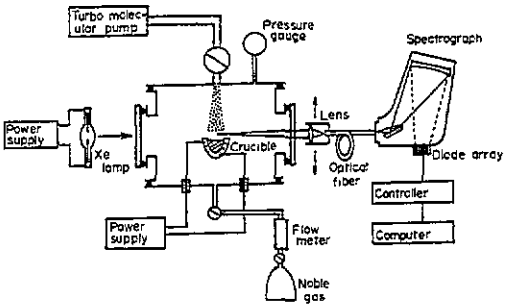


**Figure 2.** Block diagram of the time-resolved and space-resolved spectroscopy measurements.

increasing the input electrical power. After the beginning of the melting of the silver surface, the input power was kept constant. The evaporation temperature was monitored with the usual optical pyrometer. Optical spectra of selected positions in the two zones were recorded in a transmission configuration as a function of time elapsed from the beginning of the evaporation. Continuum light from a 150 W Xe lamp was directed to all the zones above the crucible through the optical window without using a lens. The transmitted light was introduced into a spectrograph (Jobin–Yvon CP-200) with a multi-channel (1024 channels) detector via a movable collecting lens and a light-fibre cable. The signals of each channel were sent to a 32-bit computer (NEC PC-9801 RS) through a controller (Atago MAX-3000). Using this optical detection system, it was possible to measure quickly a transmitted intensity spectrum at a desired height above the evaporation source in the wavelength region from 230 to 800 nm in less than 1 s, giving an effective spectral resolution of 0.57 nm. The transmission at a given height is the intensity ratio of the transmitted radiation during the evaporation process to that of the transmitted radiation through the same position before the beginning of the gas evaporation. Since the transmission $T_r$ spectra obtained contain the effects of both scattering and absorption, the results are expressed with respect to the extinction spectra, $-\log T_r$.

## 3. Results

Time-resolved extinction spectra have been measured at various positions above the evaporation source, and some typical results will now be presented. Figure 3(*a*) shows the time evolution of the extinction spectrum obtained at a representative point in the transparent region, at a height of 1.5 mm. One time-resolved spectrum consists of 32 spectra at time intervals of 0.96 s. The thirty-second spectrum is shown in figure 3(*b*). At the initial stage of the evaporation, only two sharp absorption lines $L'$ and $L''$

at about 329 nm and 339 nm, respectively, are seen. These wavelengths are close to the values of 328.07 nm and 338.29 nm reported by Choong *et al* (1966) and are due to the electronic transitions $S_{1/2} \rightarrow P_{1/2,3/2}$ in atomic silver $Ag_1$. With progressive evaporation the absorption bands below 280 nm grow. Also, faint absorption bands appear at about 355 and 430 nm and become stronger with increasing time. For the purpose of comparison with previous experimental data we enumerate the absorption bands as follows: band 1, about 249 nm; band 2 about 255 nm; band 3, about 266 nm; band 4, about 276 nm; band 5, about 355 nm; band 6, about 433 nm. Band 5 is very wide and its centre frequency is close to that of the surface plasmon of free silver microcrystals (Eversole and Broida 1977). It is therefore identified as arising from the collective oscillations of the valence electrons of the small clusters. In bands 4 and 6, fine structure characteristic of the electronic transitions accompanied by a vibrational transition is observed. Bands 1, 2, 3, 4 and 6 are assigned to the X–E, X–D, X–C, X–B, X–A transitions in silver dimers $Ag_2$, by comparison with the data of Choong *et al* (1966), who obtained these bands using a specially designed Ag discharge tube.

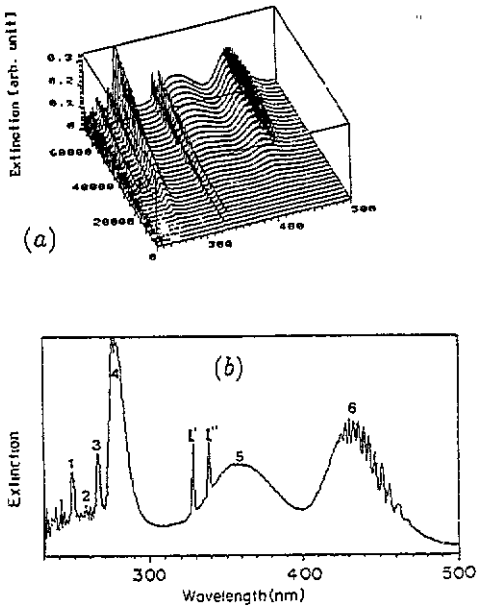


**Figure 3.** (*a*) Time-resolved extinction spectrum measured at a height of 1.5 mm from the crucible edge. (*b*) Thirty-second spectrum of the time-resolved spectrum (*a*). Bands 1, 2, 3, 4, and 6 are due to electronic-vibrational transitions of $Ag_2$. Band 5 is due to collective oscillations of the valence electrons of small $Ag_n$ clusters. The sharp lines L′ and L″ are due to the electronic transitions of $Ag_1$.

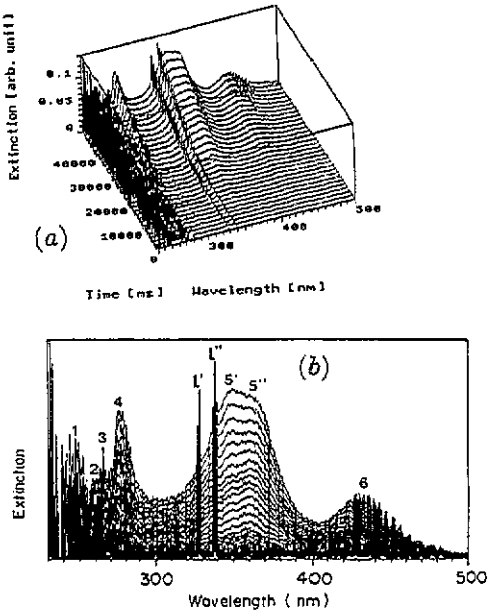


**Figure 4.** Time-resolved extinction spectrum measured at a height of 3.0 mm from the crucible edge. The band numbers and line numbers refer to figure 3 but band 5 consists of two bands 5′ and 5″ at this height.

Figure 4 shows the time evolution of the extinction spectrum measured at a height of 3 mm above the crucible. Again, at the early stages, only the atomic lines are observed and, as the evaporation proceeds, absorption bands due to $Ag_2$ and $Ag_n$ ($n > 2$) develop and increase in intensity. The plasmon band of $Ag_n$ is seen

to consist of two broad adjacent bands 5′ and 5″ centred at 348 nm and 361 nm, respectively. Some intensity competition between these two subbands is observed; at the early stages the 361 nm band dominates, but later the 348 nm band grows more rapidly and becomes stronger.

Figure 5(*a*) shows the time evolution of the extinction spectrum measured at a height of 6 mm above the crucible, which is near the boundary of the transparent zone. Initially, only the atomic lines appear, and later the absorption bands due to $Ag_2$ and $Ag_n$ clusters increase in intensity. The thirty-second (and last) spectrum is shown in figure 5(*b*). The atomic lines and the various dimer lines still exist, but the plasmon band at about 355 nm has become strong and very wide.

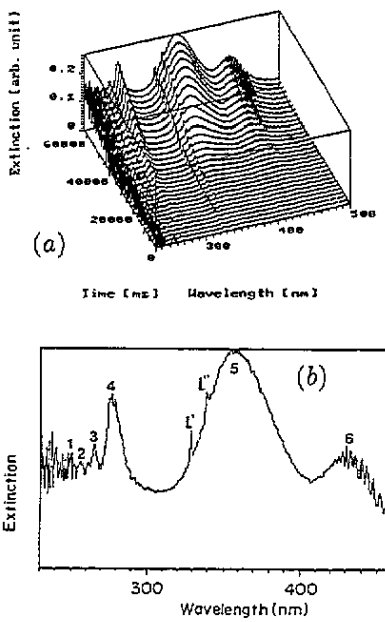


**Figure 5.** (*a*) Time-resolved extinction spectrum measured at a height of 6.0 mm from the crucible edge. (*b*) Thirty-second spectrum of the time-resolved spectrum (*a*). The band numbers and line numbers refer to figure 3.

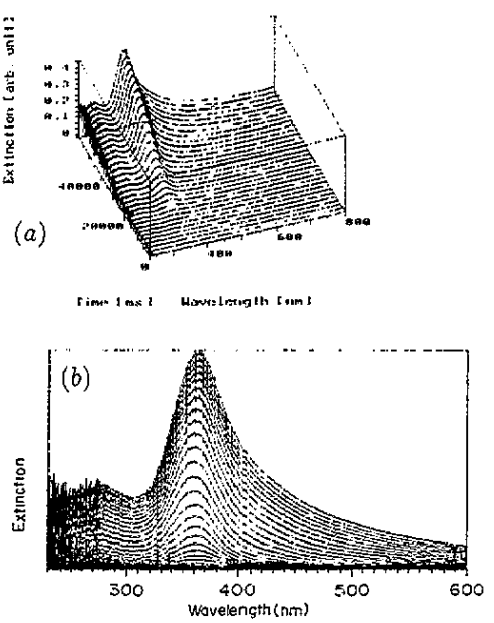


**Figure 6.** Time-resolved extinction spectrum measured at a height of 10 mm from the crucible edge.

Figure 6 shows the time evolution of the extinction spectrum measured at a height of 10 mm, which is in the lower part of the smoky zone. At the beginning of the evaporation the atomic lines are still observed, and with progressive evaporation the microcrystal plasmon band dominates the spectrum. It is asymmetrical, with a shoulder on the long-wavelength side. Also, the interband absorption characteristic of bulk Ag is already well established in the wavelength region below about 310 nm.

Figure 7 shows the time evolution of the extinction spectrum at a height of 23 mm above the crucible, which is in the upper part of the smoky region. In this region the spectra are due to large clusters and microcrystals, and no atomic lines are observed. At the initial stage the plasmon band appears at 352 nm and shifts to longer wavelengths with an accompanying shoulder at long wavelengths. With progressive evaporation the plasmon peak shifts to longer wavelengths and the asymmetry is enhanced.

All the spectra shown so far were recorded in a confined helium gas, at a pressure of 140 Torr. We have also performed measurements in flowing helium gas, with a flow rate of 0.6 litre $min^{-1}$, at a pressure of 3 Torr. Spectra obtained with this method are shown in figure 8. At the initial stage a broad band appears at about 352 nm, and with progressive evaporation the band becomes sharper and the wavelength shifts to 359 nm. Although we cannot determine the size of the free microcrystals directly, electron microscope examination of the microcrystals collected on a substrate showed that their average size was about 10 nm.

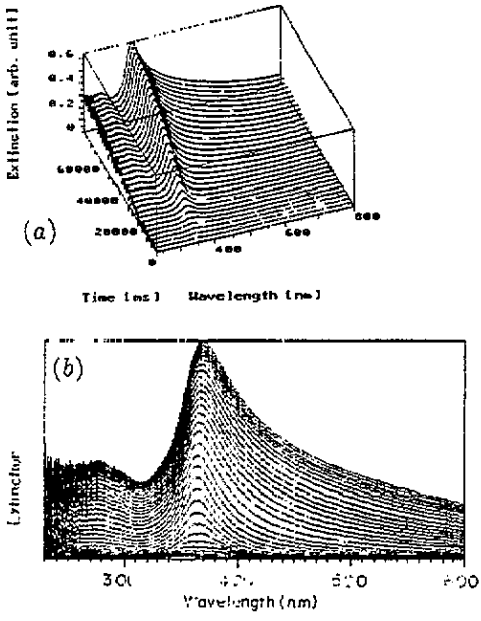


**Figure 7.** Time-resolved extinction spectrum measured at a height of 23 mm from the crucible edge.

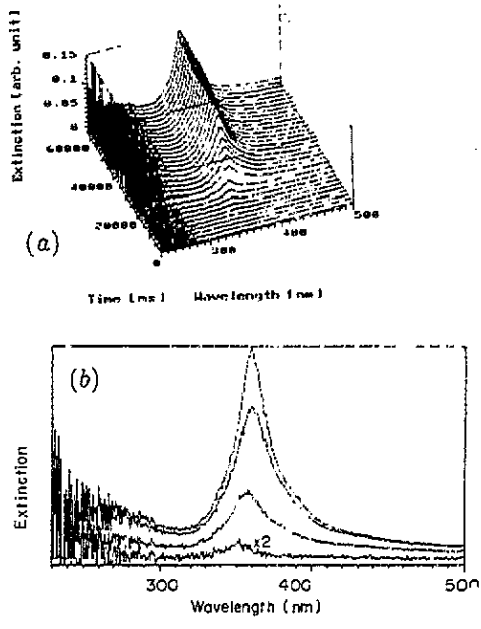


**Figure 8.** (*a*) Time-resolved extinction spectrum measured at a height of 3.0 mm from the crucible edge under the flowing-gas condition. (*b*) Tenth, fifteenth and thirty-first spectra of (*a*).

## 4. Discussion

The assignments of the various absorption bands have already been presented with the experimental results, and we now discuss some of the features of the spectra in more detail. We note first that the observed $Ag_2$ spectra are qualitatively similar to those obtained with the matrix isolation technique (Welker and Martin 1979, Schulze *et al* 1987) but also show a fine sharp phonon structure. This implies that the vibrational damping is enhanced in the presence of a crystalline host lattice. The absorption wavelengths observed in the present study differ from those observed with a matrix isolated specimen, and this is due to the perturbations and deformations caused by the host lattice.

We discuss some of the features of band 5, the plasmon band. At a height of 3 mm (figure 4) the plasmon absorption was found to consist of two broad adjacent bands. Since we do not know the sizes and the polarizabilities of the Ag clusters

which produce this double peak, we cannot perform a theoretical calculation of this spectrum. There seem to be two possible mechanisms for the double-peak structure.

(1) Spheroidal clusters exist which are characterized by two absorption frequencies corresponding to the cases of the incident field parallel to the long and short axis, respectively. A splitting of this type was observed in the photoabsorption cross section of very small Na clusters containing fewer than 20 atoms (Selby *et al* 1989).

(2) Various $Ag_n$ clusters coexist, but with the predominance of two specific types: $Ag_{n'}$ and $Ag_{n''}$. Ion mass spectrometry of silver clusters (Katakuse *et al* 1985) has shown that stable clusters occur at the magic numbers $n$ = 2, 8, 20, 34, 40, 58, 92, 138 and 198. For clusters of these sizes the resonance frequency is size dependent. Thus, if, owing to the high temperature in the transparent region, larger clusters are decomposed into small clusters with two predominant sizes, a double-peak structure may appear.

At larger heights above the crucible and at later times, the broad plasmon band dominates the spectrum and has a long-wavelength tail (figures 6 and 7). The tail is due to interactions between adjacent microcrystals, as we now demonstrate by calculations of the absorption spectrum of two interacting Ag spheres, applying a method based on the use of bispherical coordinates (Ruppin 1989). The optical constants of silver were taken from the experimental data of Johnson and Christy (1972). These, however, refer to the bulk and for small spheres have to be modified so as to account for the limitation of the electron mean free path (Kreibig and Fragstein 1969). We introduce this size correction in the form suggested by Kreibig (1974), according to which the dielectric constant of a sphere of radius $R$ is given by

$$\epsilon(\omega, R) = \epsilon_{1b}(\omega) + i[\epsilon_{2b}(\omega) + (\omega_p^2/\omega^3)(v_F/R)].$$

Here $\epsilon_{1b}$ and $\epsilon_{2b}$ are real and imaginary parts of the bulk dielectric constant. $\omega_p = 1.38 \times 10^{16}$ s$^{-1}$ is the plasma frequency and $v_F = 1.4 \times 10^6$ m s$^{-1}$ is the Fermi velocity. In figure 9, the calculated absorption cross section of pairs of Ag spheres which are randomly oriented with respect to the incident wave polarization direction is shown for three inter-particle distances. It is found that the interaction between the spheres causes a splitting of the absorption band into two peaks. The low-frequency peak moves to longer wavelengths with decreasing inter-particle distance, while the high-frequency peak hardly shifts. Thus, in an experimental situation in which there exists a range of inter-particle distances, we expect a long-wavelength tail to be formed. We note that Hayashi *et al* (1990) have also observed such a tail in the spectra of gas-evaporated Ag microcrystals collected on glass plates and correctly identified it to result from interactions between the crystallites.

The behaviour of the plasmon band observed in the flowing-gas condition (figure 8) is completely different. The band becomes sharper with increasing time. In this case there is no broadening due to inter-particle interaction. With increasing time, larger crystallites are formed and the band becomes narrower because the size-dependent damping term decreases. From the experimentally observed widths we can estimate the sizes of the microcrystals corresponding to the various spectra. Thus, for example, for the tenth, fifteenth and thirty-first spectra of figure 8(*a*), shown separately in figure 8(*b*), we have found that the corresponding sphere diameters are 4.3 nm, 5.4 nm and 7.6 nm. The absorption spectra calculated for these sphere sizes

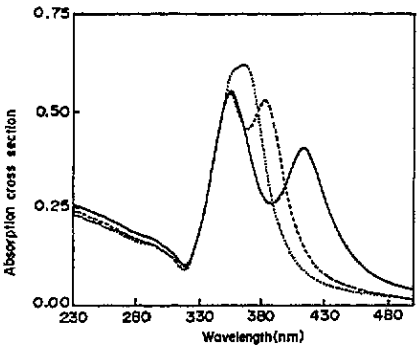


**Figure 9.** Calculated absorption cross sections (in units of the geometric cross section) of pairs of Ag spheres with a radius of 3 nm. The full, broken, and dotted curves were obtained by assuming that the inter-particle distances are 0.2 nm, 0.5 nm and 1.0 nm, respectively.

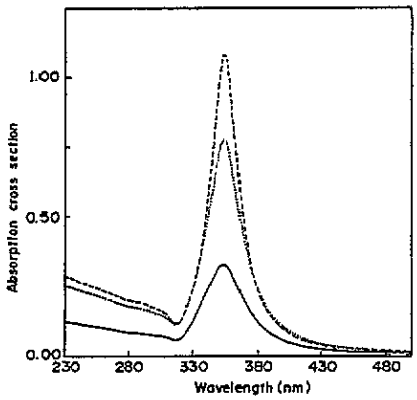


**Figure 10.** Calculated absorption cross sections of Ag microcrystals. The full, dotted, and broken curves were obtained for radii of 4.3 nm, 5.4 nm and 7.6 nm, respectively.

are shown in figure 10. Since we do not know the density of the microcrystals in the experiment, we have adjusted the relative peak heights so as to agree with the measured intensity ratios.

The time-resolved and space-resolved spectra provide some information about the cluster growth process. Figure 11 shows the time dependence of the extinctions due to atoms ($Ag_1$), dimers ($Ag_2$) and clusters ($Ag_n$) at various heights, where each curve is normalized to its maximum value. The extinction is proportional to the number for $Ag_1$ and $Ag_2$ while for $Ag_n$ it depends on both the number of the clusters and their sizes. At heights of 1.5 and 3 mm, the extinction due to all species increases almost steadily with time. At a height of 6 mm, the number of atoms increases with time and then, after reaching a maximum, begins to decrease, while the extinction due to clusters continues to increase. This indicates that clusters grow by coalescence with atoms. With increasing height, the decrease in the extinction due to $Ag_1$, after the maximum, becomes more prominent. These results indicate how the well separated zone structure above the evaporation source (figure 1) is formed. Clusters of various sizes first appear near the evaporation source and migrate upwards by convection. The clusters tend to grow by coalescence with surrounding atoms or clusters. However, clusters near the evaporation source are heated so intensely that they tend to fission as follows. Generally, clusters suffer shape distortions due to collisions with atoms or other clusters or due to structural fluctuations. The distortions are restored by the surface tension and the clusters oscillate in shape (as in the liquid drop model for nuclei). Close to the evaporation source the temperature is so high that the distortions overcome the surface tension and the clusters split into smaller clusters. Higher above the source the temperature is lower and cluster growth prevails against fission, which gives rise to the formation of the smoky zone. In the confined high-pressure gas condition, the smoky zone is compressed by the cold noble gas near the chamber wall, thus becoming conical in shape as shown in figure 1. Also, we note that, since no emission is observed from the smoky zone without illumination, the clusters are cooled not by photoemission but by collisions with noble-gas atoms.

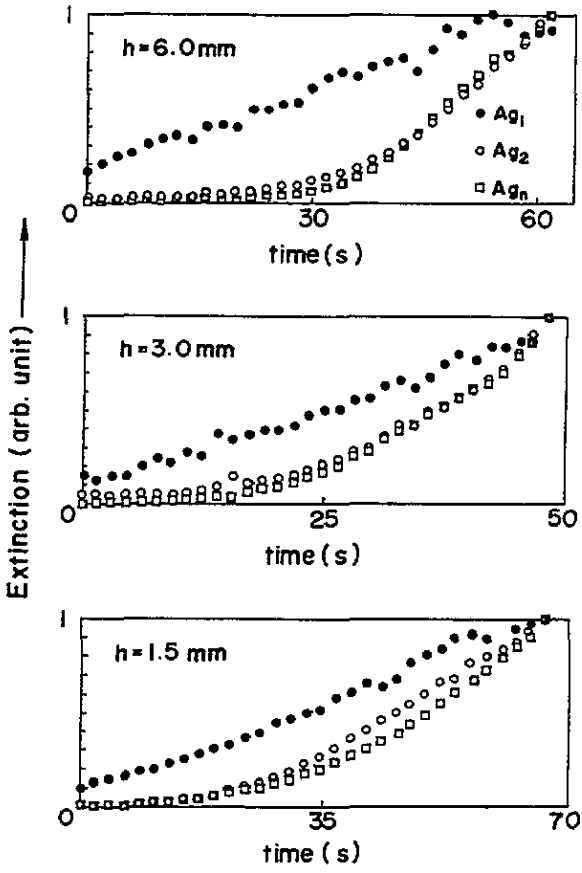


**Figure 11.** Time dependence of the extinction at various heights ($h$) from the upper edge of the crucible.

In conclusion, we have presented a technique for characterizing *in situ* and without any substrate effect the optical properties of metallic species (which may be atoms, clusters or microcrystals) during their formation by thermal evaporation and with residual pressure of an inert gas. The main limit of the technique is that there is no direct characterization of the cluster size. Bearing this limit in mind, we have presented a reasonable connection between measured optical data and the existence of atoms, clusters and microcrystals, with a convincing coherence with the results from the literature.

## Acknowledgments

This study was supported in part by a Grant-in-Aid for Scientific Research from the Ministry of Education (Japan). This study was also supported in part by a Grant-in-Aid (1991) for Overseas Research from Nihon University. The authors acknowledge Mr Hiroshige Siota and Mr Norimichi Takayama for assistance in constructing the experimental system and the measurements.

## References

Choong S P, Wang L S and Lim Y S 1966 *Nature* 209 1300

Eversole J D and Broida H P 1977 *Phys. Rev.* B **15** 1644
Granqvist C G and Buhrman R A 1976 *J. Appl. Phys.* **47** 2200
Hayashi S, Koga R, Ohtuji M and Yamamoto K 1990 *Solid State Commun.* **76** 1067
Hayashi T, Ohno T, Yatuya S and Ueda R 1977 *Japan. J. Appl. Phys.* **16** 705
Johnson P B and Christy R W 1972 *Phys. Rev.* B **6** 4370
Katakuse I, Ichihara T, Fujita Y, Matuo T, Sakurai T and Matsuda H 1985 *Int. J. Mass Spectrom. Ion Processes* **67** 22
Kreibig U 1974 *J. Phys. F: Met. Phys.* **4** 999
Kreibig U and Fragstein C V 1969 *Z. Phys.* **224** 307
Mochizuki S 1991 *Phys. Lett.* **155A** 510
—— 1992 *Phys. Lett.* **164A** 191
Ruppin R 1989 *J. Phys. Soc. Japan* **58** 1446
Saito Y 1989 *Japan. J. Appl. Phys.* **28** L2024
Schulze W, Becker H U and Abe H 1978 *Chem. Phys.* **35** 177
Selby K, Vollmer M, Masui J, Kresin V, de Heer W A and Knight W D 1989 *Phys. Rev.* B **40** 5417
Ueda R 1974 *J. Cryst. Growth* **24–5** 69
Welker T and Martin T P 1979 *J. Chem. Phys.* **70** 5863